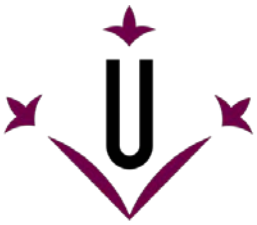

An experimental study of a new hybrid jet impingement / micro-channel cooling scheme

Jérôme Barrau (1), Daniel Chemisana (1), Joan Rosell (1), Lounes Tadrist (2), M. Ibañez (1)

(1) Universitat de Lleida (Spain), Edifici CREA, C/Pere de Cabrera, s/n

(2) IUSTI, Techn. de Château-Gombert, 5 rue Enrico Fermi – 13453 Marseille Cedex 3

jerome@macs.udl.cat; daniel.chemisana@macs.udl.cat; rosell@macs.udl.cat; lounes.tadrist@polytech.univ-mrs.fr; m.ibanez@macs.udl.cat

ABSTRACT

A new hybrid cooling scheme is proposed for high heat flux management and power devices. This scheme combines the benefits of micro-channel and jet impingement cooling technologies, with the additional objective of improving the temperature uniformity of the cooled object. The geometry is tested experimentally to characterize its performances and to assess its capacity to provide this characteristic. The temperature distribution of the heat sink has been measured through a matrix of thermocouples. The hybrid cooling scheme is shown to have the capacity to optimize the temperature uniformity of the cooled object, since the experimental design provides a global decrease of the temperature of the heat sink in the direction of the fluid flow.

Keywords

Jet impingement; Microchannel; Heat sink; Temperature uniformity

Nomenclature

A_t	area of aluminium block's top test surface (m^2)
C_p	specific heat ($J/kg \cdot K$)
d_h	hydraulic diameter (m)
ΔP_{in-out}	pressure losses between the inlet and the outlet of the heat sink (Pa)
ΔT_{in-out}	temperature difference of the fluid between the inlet and the outlet of the heat sink (K)
h_l	local heat transfer coefficient ($W \cdot m^2/K$)
k	thermal conductivity (W/m.K)
L	length (m)
R	thermal resistance coefficient ($K \cdot m^2/W$)
T	temperature (K)
T_S	temperature of the surface to cool (K)
T_F	temperature of the fluid in the exchange interface (K)
T_{in}	inlet temperature of the refrigerant fluid (K)
T_{out}	outlet temperature of the refrigerant fluid (K)
T_W	average temperature on the wall in which is applied the heat flux (K)
P_f	power absorbed by the refrigerating fluid (W)
P_W	power delivered by the feeding source (W)
q''	heat flux (W/m^2)
q''_{eff}	effective heat flux based on top test surface area of aluminium block, $q''_{eff}=P_i/A_t$ (W/m^2)
Q	flow rate (m^3/s)
v	velocity (m/s)
W	width (m)
x	horizontal position (m)
y	transversal position (m)
z_0	vertical position of the bottom of the heat sink (m)
z	vertical position (m)

Greek symbols

ξ	form factor
ρ	density (kg/m^3)
σ_T	standard deviation of the temperature of the bottom of the heat sink (K)
υ	kinematic viscosity

Subscripts

Al	Aluminium
f	fluid
i	row number of the thermocouples matrix
j	longitudinal section number of the thermocouples matrix
jet	jet
l	local
m	average value
min	minimum
max	maximum
s	test surface; solid

1 Introduction

Several studies have been published on the fluid flow and heat transfer characteristics of single-phase high heat flux removal schemes. These cooling schemes, which use micro-channel and jet impingement systems, are commonly employed in the cooling of high-performance microprocessors, laser diode arrays, radars, X-ray anodes, and solar photovoltaic concentrators. Micro-channel and jet impingement schemes have recently been compared [1-2] and are the object of constant developments. Both technologies provide very high flux removal, but still present serious drawbacks. Micro-channels cause a large increase in temperature along the path of the fluid flow and are also responsible for a relatively large pressure drop. Jet impingement requires the use of numerous jets to ensure a relatively good level of uniformity of temperature across the base of the heat sink. These cooling schemes have the disadvantage of reducing the local heat transfer coefficient because of the interaction between adjacent jets. The solution to this problem lies in the use of complex geometries that allow the extraction of the spent flow from the jets. Many studies have attempted to reduce these effects [3-5] and at the same time to enhance the heat transfers associated with the two technologies.

Temperature non uniformities in micro-channels or jet impingement cooling affect the performance of electrical systems and causes mechanical stresses due to the difference of thermal expansion from one side to the other of the cooled object. Both factors reduce the reliability of the whole system. As a consequence, main research on heat sinks focuses on improving the resistance of the devices to thermal cycles, matching the thermal expansion coefficient of the "packaging" to the one of semiconductors. Another way of investigation is to improve the temperature uniformity of the cooled object.

To date, few works have been published about hybrid systems in which the benefits of micro-channel and jet impingement are combined to overcome the main drawbacks associated with the two techniques. Jang et al. [6]

experimentally investigated a micro-channel heat sink subjected to an air impinging jet. They demonstrated that, under certain specific conditions, the efficiency of cooling was 48.5% better than that achieved applying a classical micro-channel design, with pressure losses being reduced by 90.5 %. The manifold micro-channels developed by Copeland et al. [7] and optimized by Ryu et al. [8] is another technology that has a similar effect to that of impinging jets on a micro-channel heat sink.

The combination of both technologies in hybrid cooling schemes makes it possible to significantly increase thermal exchange within the cooling system. In effect, this design allows to reduce the length of the flow circuit by the half in the dissipation system. This is important, as indicated by Lee and Vafai [9], since an increase in the length of the flow circuit causes a reduction in the maximum quantity of heat that can be extracted by the system, whether through micro-channels or through jet impingement devices. Furthermore, this shortening of the flow circuit implies a reduction in pressure losses within the system [10]. An other important feature of jet impingement / micro-channel hybrid systems studied in the literature is that they were shown to improve the uniformity of the temperature of the cooled surface. Sung and Mudawar [11-12] analyzed hybrid jet impingement / micro-channel cooling schemes both experimentally and numerically (Fig. 1) and conclude that the hybrid modules maintain a higher degree of surface temperature uniformity than other cooling scheme.

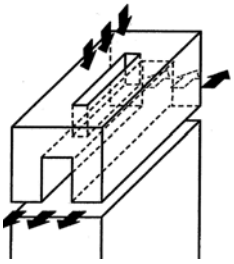

Fig. 1. Hybrid jet impingement /micro-channel cooling system by Sung and Mudawar [11]

In this study, a new hybrid cooling scheme is experimentally evaluated. This scheme involves feeding coolant from a slot jet in a modified micro-channel heat sink structure. Experimental analysis is used to study the main trends of the heat exchanges of the hybrid cooling scheme and to assess the capacity of the heat sink to improve a high temperature uniformity of the cooled object.

2 Controlled temperature hybrid jet impingement microchannel cooling scheme

2.1 Conceptual analysis

In all cooling schemes, the temperature of the refrigerating liquid (T_f) increases throughout the circuit as a result of the absorption of energy. In the case of micro-channels, the heat transfer coefficient remains constant throughout the whole heat sink due to the geometry of the system while impinging jets offer a characteristic global reduction in the heat transfer coefficient along the circuit. However, as the energetic flux (q") that arrives at

the cooling system is generally uniform, the temperature at the base of the heat sink ($T_{S,l}$) increases in the direction of the fluid flow.

The local heat transfer coefficient (h_l) is calculated from equation (1):

$$h_l = \frac{q''_l}{T_{S,l} - T_{f,l}} \quad (1)$$

The local temperature of the bottom of the heat sink can be extracted from equation (1):

$$T_{S,l} = \frac{q''_l}{h_l} + T_{f,l} \quad (2)$$

Analyzing this equation, it is evident that increasing the heat transfer coefficient throughout the circuit is the only way to obtain a uniform temperatures pattern on the heat sink's base (T_S).

In both micro-channels, and impinging jets, thermal exchanges vary according to the regime of the flow and the geometry of the circuit. For a given design, the flow regime remains fixed by the fluid velocity and the inlet section of the heat sink. Therefore, the only way to increase the heat transfer coefficient is to develop a cooling scheme with a variable internal geometry in the direction of the coolant flow.

2.2 Design description

On the base of the bibliographic analysis of the different parameters of cooling systems involving micro-channels and impinging jets, a new design is proposed (Fig. 2).

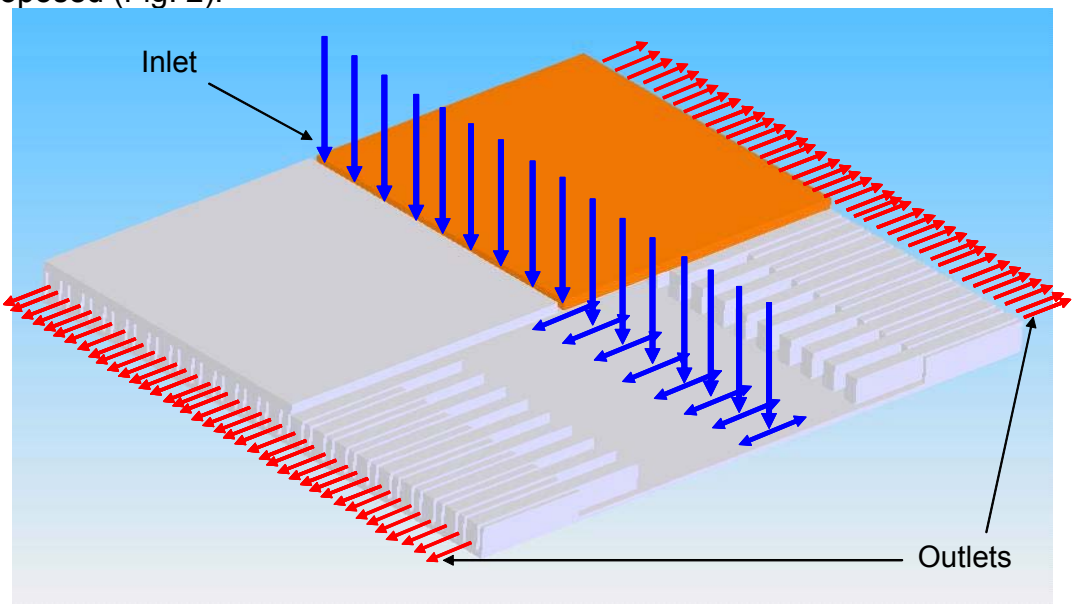

Fig. 2. Proposed design (linear symmetry)

In this scheme, fluid enters through the slot located in the symmetry plane of the heat sink (arrows in blue), between the two upper plates (which were cut in order to enable us to observe the geometry of the system) and leaves it through the extremities of the channels (arrows in red). Between entering the heat sink and subsequently exiting it, the fluid flows through a series of micro-

channels with a variable longitudinal distribution. The linear symmetry of the system means that both the entry and exit of the liquid are simpler than under conditions of circular symmetry. Furthermore, this guarantees the symmetry of thermal exchange in one dimension.

This design entails two well differentiated areas. The first corresponds to a cooling system using jet impingement, while the second relates to a system of micro-channels. The relative arrangement of the channels with regard to the impact area of the fluid defines the degree of interaction between the two types of thermal exchange.

Besides combining different characteristics that directly influence local heat transfer coefficients, this system constitutes a change from the matrices of impinging jets and also from the hybrid jet impingement / micro-channel system suggested by Sung and Mudawar [11]: In effect, in both types of cooling system, the flows from adjacent jets meet head on, implying a major deceleration of flow and even points where fluid flow stops and becomes stationary. In the proposed design, the radial acceleration of the fluid that impacts against the surface to cool, which is an essential aspect of the physics of thermal exchange at jet impingement heat sinks, is free.

3 Experimental Set up

3.1 Experimental device

The relatively high thermal conductivity of aluminium (k_{Al} =237 W/m.K at 300 K) and the simplicity of its mechanization led us to make the experimental device using this material (Fig. 5). The upper platform of the experimental heat sink, which corresponds to the area of the system to be cooled, measures 2.55 cm (width) by 5.95 cm (length). The depth of the micro-channel, which are fitted at the top of the heat sink, is 2.5 mm. Their widths vary at different points along the refrigerating liquid circuit, ranging from 3.5 mm to 0.5 mm, with an intermediate section in which the channel width is 1.5 mm. The fins, which serve as vertical walls in the micro-channels, are 0.5 mm wide.

In the lower part of the system, a housing to every part end was added, in order to introduce electrical resistances that simulate energy that must be extracted by the heat sink. These housings are separated from the bottom of our dissipation system by a thickness of 23 mm that made it possible to homogenise the thermal flow within the mass of material and thereby ensure that it arrives at the point of thermal exchange with the refrigerating liquid in as uniform a state as possible.

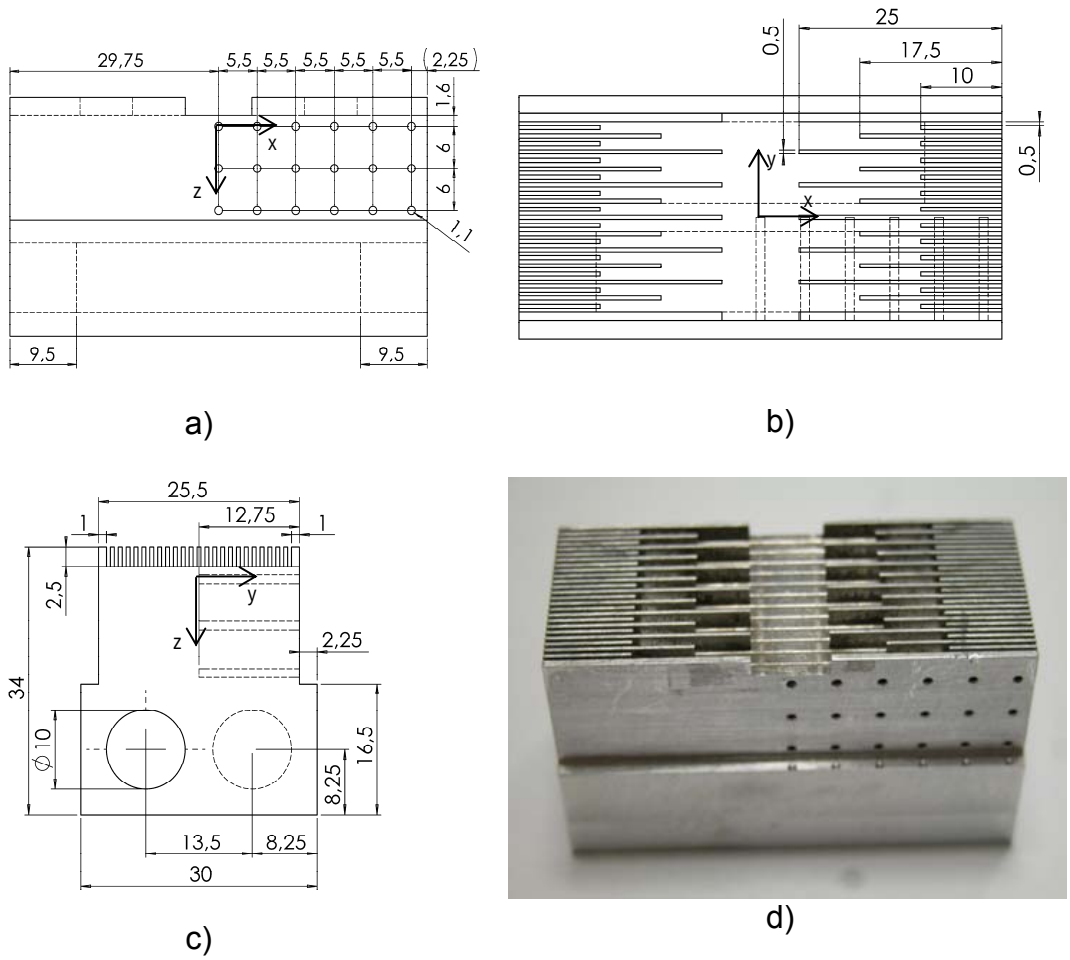

Fig. 3. Schemes and photography of the experimental part. a) Front view, b) Upper View, c) Side view, d) photography

As shown in Fig. 3, the 18 1.1 mm diameter drill holes observed in the front view of the device, under the bottom of the heat sink, are used to house the 1 mm diameter type K thermocouples (Chromel-Alumel). The depth of these drill holes is half the width of the experimental heat sink in order to measure the temperature of the system along the longitudinal plane of symmetry of the device.

At the top of the experimental heat sink, the refrigerating liquid distributor in our cooling system is formed by a single Plexiglas part composed of three volumes:
- One entry volume, which guides the refrigerating liquid to the area of the jet impingement of the heat sink through a slot in its bottom.
- Two exit volumes, which collect the liquid leaving the micro-channels at the extremities of the heat sink.

The lower face of this part, which is in contact with the fins of the heat sink, is used to create the closed micro-channels through which the refrigerating liquid flows. Drill holes were made in each of the three volumes of the space used for distributing the refrigerating liquid in order to allow the introduction of pressure and temperature sensors. Finally, a Plexiglas cover was fitted to the top of the distributor hall with a drill and tightened onto each of the three volumes in order to receive the connectors of the hydraulic circuit.

3.2 *Experimental mount*

The experimental device was then secured to a desk using a support made with an insulating material (Bakelite). The rest of the experimental model was insulated using rock wool.

The hydraulic circuit is designed to provide temperature, pressure and flow control at the point at which the refrigerating liquid enters in the system (Fig. 4). The 3 pressure sensors are located in both exit volumes and in the entry one.

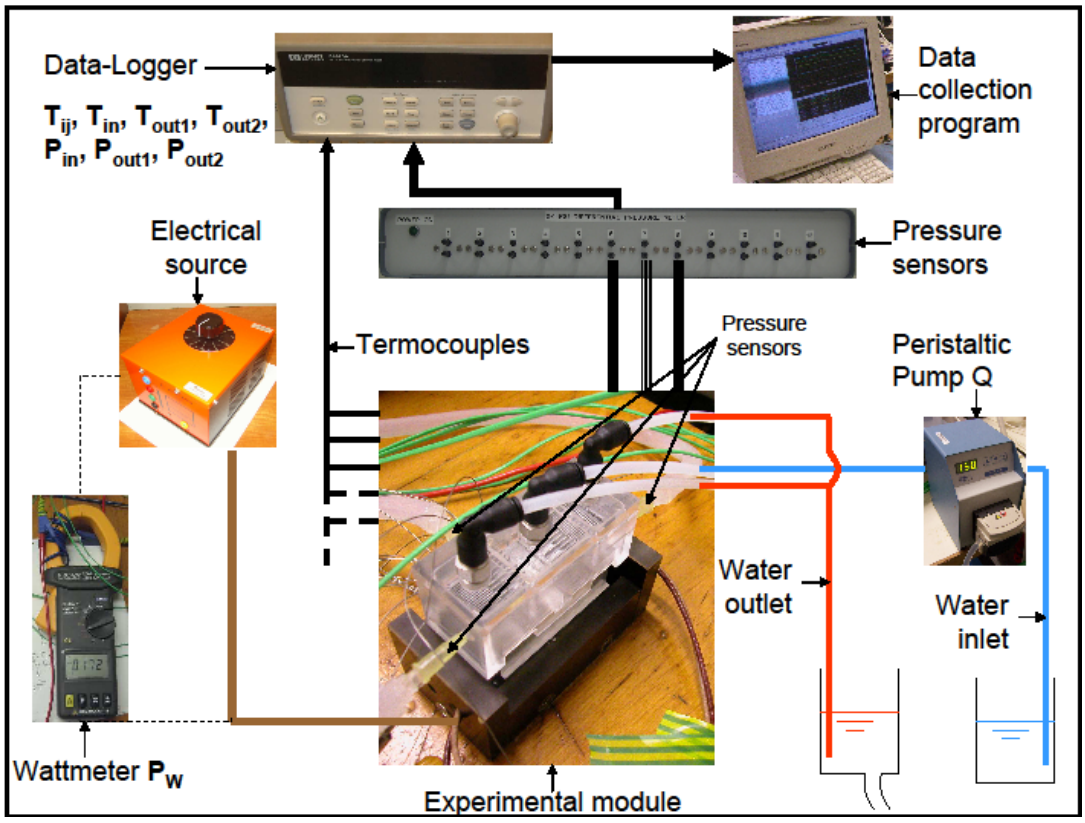

Fig. 4. Experimental set up

In order to obtain temperatures from the bottom of the dissipation system from several sections along the fluid circuit ($T_{zo,j}$ with j=0,1,2,3,4,5) without intrusive measurements that disturb the flow and consequently invalidate any results obtained, the methodology described by Robinson and Schnitzler [13] was used. Vertical series of thermocouples with known vertical and transversal positions were located in every section where the measurement of the temperature at the bottom of the heat sink was planed (Fig. 5). This matrix of thermocouples (T_{ij}, with i=1, 2, 3 and j=0, 1, 2, 3, 4, 5) allows determining the temperature at the bottom of each section through the following calculation:

$$T_{z_0,j} = T_{1j} + (z_{0j} - z_{1j}) \cdot \left(\frac{T_{ij} - T_{1j}}{z_{ij} - z_{1j}} \right) \text{ for } \begin{cases} i = 2 \text{ or } i = 3 \\ \text{and} \\ j = 0,1,2,3,4,5 \end{cases} \quad (3)$$

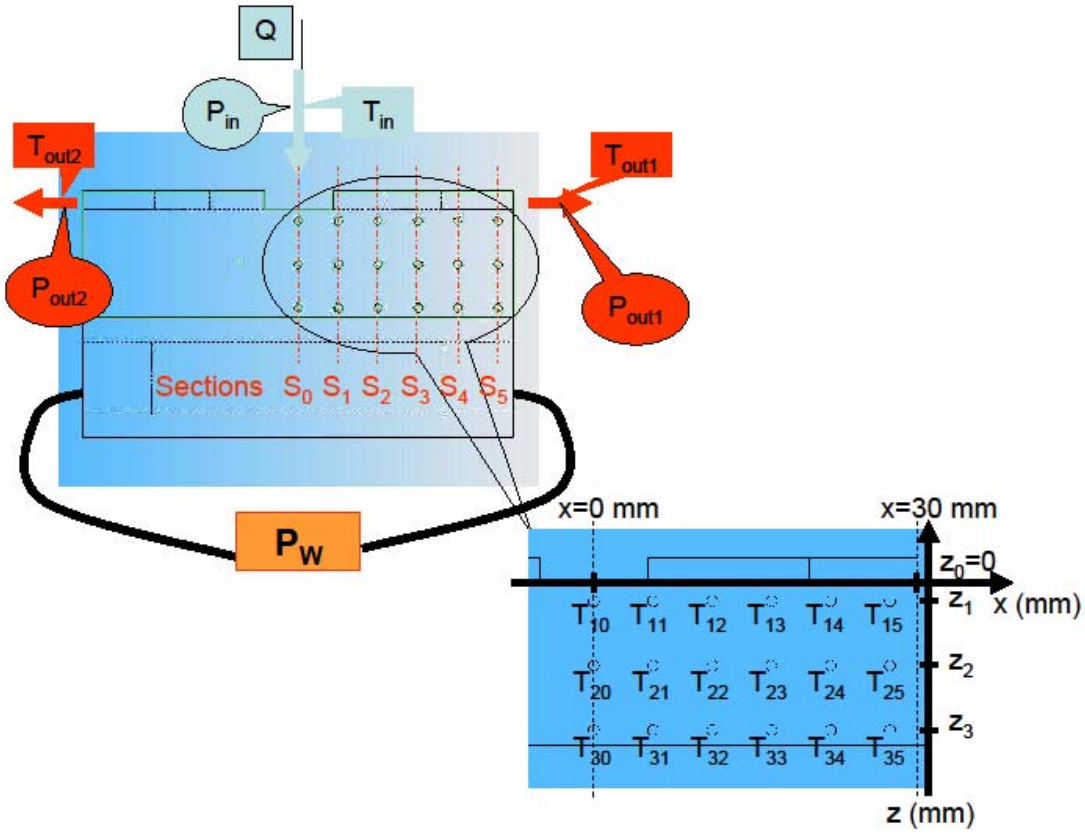

Fig. 5. Controlled parameters of the experimental module

The uncertainties in flow rate measurements, pressure levels, electrical power levels and temperatures were ±2%, ±1%, ±10 W and ±0.2 ºC, respectively.

4 Results and discussion

4.1 Energy Balance

A sequence of measurements was considered valid if the energy balance of the system was verified: all the power delivered by the feeding source (P_i) and therefore transferred, in the form of heat, to the experimental model through the resistances, must have been absorbed by the refrigerating liquid (P_f). This power is calculated through the expression:

$$P_f = \rho_{water} \cdot Cp_{water} \cdot Q \cdot \left(T_{out} - T_{in}\right) \quad (4)$$

At the end of the calculations, the energy balance is verified if:

$$P_f = P_W \quad (5)$$

The results of the energy balance can be presented in terms of the observed difference in the temperature of the refrigerating liquid between the inlet and the outlet of the heat sink (T_{out}-T_{in}) and the Reynolds number. The section through which the fluid enters the heat sink is an elongated slot with a form factor ξ defined by the expression:

$$\xi = \frac{W_{jet}}{L_{jet}} \tag{6}$$

In such sections, the hydraulic diameter is calculated according to:

$$d_h = \frac{2 \cdot W_{jet}}{1 + \xi} \tag{7}$$

The Reynolds number is calculated using the expression:

$$Re = \frac{v.d_h}{\upsilon} \tag{8}$$

The conditions for the seven validated tests are presented in table 1.

Table 1
Tests conditions

		TEST 1	TEST 2	TEST 3	TEST 4	TEST 5	TEST 6	TEST 7
T_{in}	ºC	12.35	12.35	12.59	12.73	12.5	12.7	29.2
Q	m^3/s	2.07E-05	2.07E-05	1.32E-05	8.42E-06	1.55E-05	1.55E-05	1.60E-05
q''_{eff}	W/cm^2	21.8	32	31	31	13.2	31	32

Fig. 6 compares the measured water temperature rise between the channel inlet and outlet, and theoretical values predicted from the simple energy balance. The excellent agreement between the two proves virtually all the electrical power supplied by the cartridge heaters was removed by the water, and heat losses are indeed negligible.

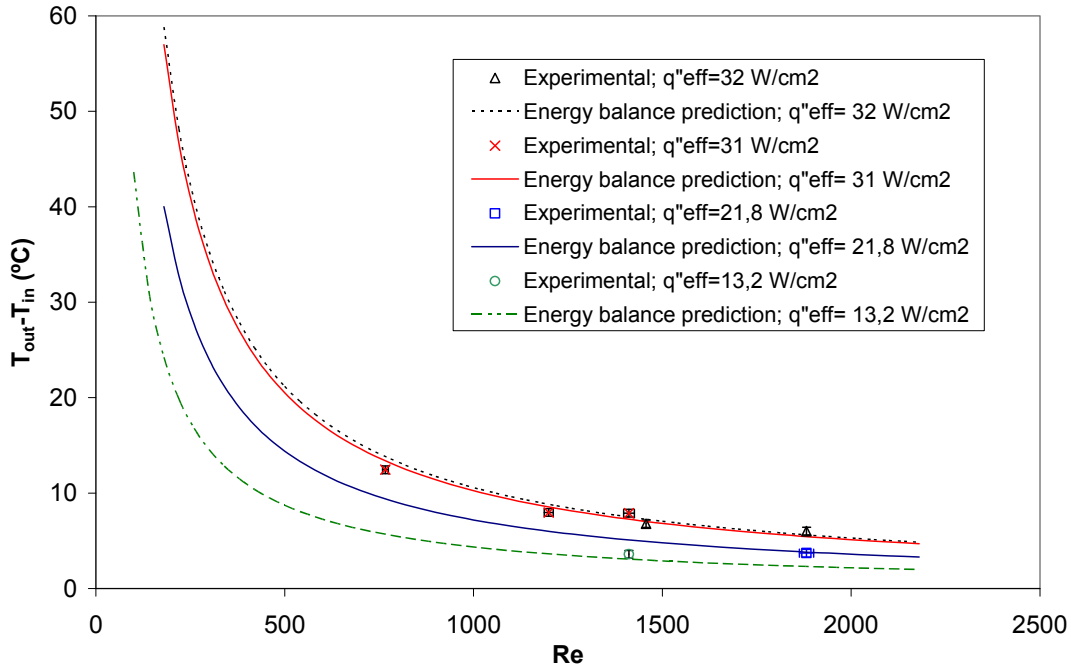

Fig. 6. Comparison of experimental data and energy balance predictions for water temperature rise from heat sink inlet to outlet

4.2 Temperature maps

The qualitative observation of the evolution of temperature at the bottom of the heat sink, for the different test conditions, indicates that the studied cooling scheme solves one of the features initially suggested as a design criterion (Fig. 7). Indeed, the temperature at the bottom of the heat sink shows an overall downward slope throughout the fluid circuit, indicating that by optimizing the parameters of the design, it is possible to achieve a uniform temperature throughout the heat sink. The average temperature at the bottom of the heat sink ($T_{z0,m}$) is calculated by the equation:

$$T_{z0,m} = \frac{T_{z0,j=0} + \sum_{j=1}^{5} 2 \cdot T_{z0,j}}{11} \qquad (9)$$

where $T_{z0,j}$, for j = 0, 1, 2 , 3 , 4 ,5 are the temperatures at the bottom of the heat sink in the experimental module sections S_0, S_1, S_2, S_3, S_4 y S_5 respectively.

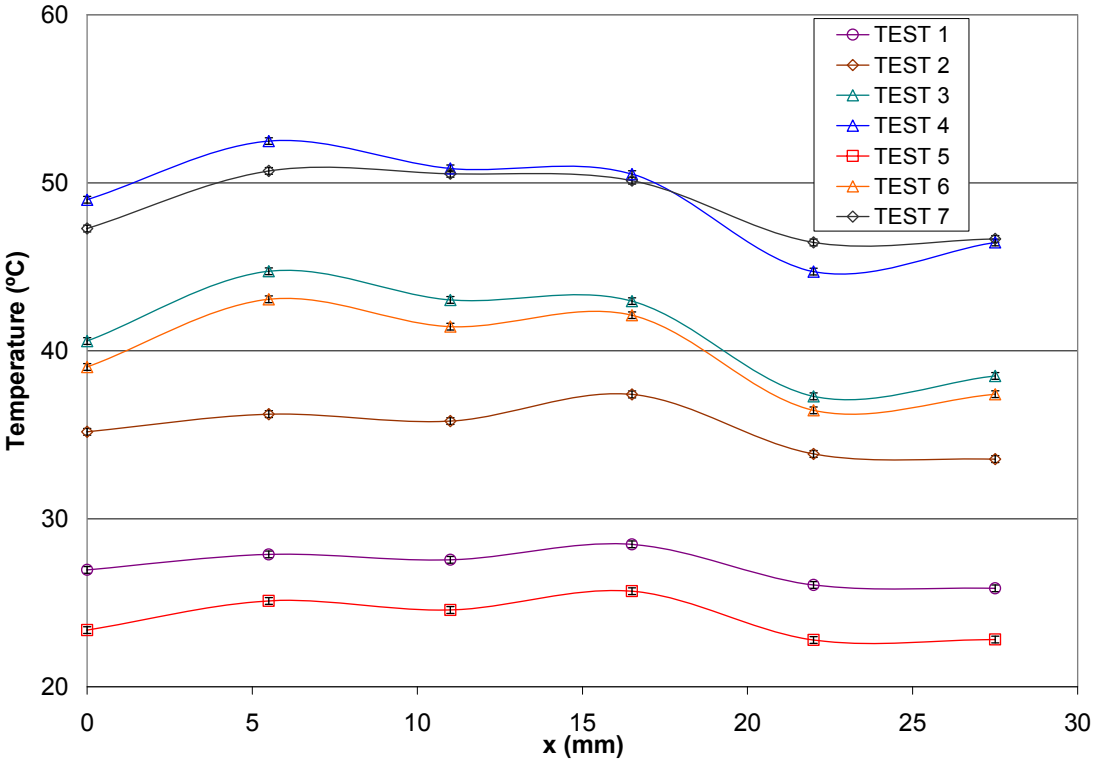

Fig. 7. Temperature maps of the experimental heat sink. Every point contents uncertainty bars according to the accuracy of the sensor.

Table 2 presents results for temperature uniformity at the bottom of the heat sink. They are expressed by the standard deviation (σ_T) with respect to average temperature and by the maximum temperature difference on this surface.

Table 2
Temperature uniformity at the bottom of the heat sink

Symbol	Unit	TEST 1	TEST 2	TEST 3	TEST 4	TEST 5	TEST 6	TEST 7
$\Delta T_{in\text{-}out}$	ºC	3.7	6.0	8.0	12.5	3.6	7.9	6.8

Heat sink bottom	$T_{z0,m}$	ºC	27.1	35.4	39.4	47.3	24.4	41.0	48.7
	$T_{z0,min}$	ºC	25.9	33.6	36.5	43.8	22.8	37.4	46.4
	$T_{z0,max}$	ºC	28.5	37.4	42.6	49.8	25.7	43.1	50.7
	$\Delta T_{min-max}$	ºC	2.6	3.8	6.1	6.0	2.9	5.7	4.3
	σ_T	ºC	1.0	1.5	2.4	2.3	1.2	2.3	1.9

The temperature uniformity does not decrease linearly with regard to differences in the temperature of the fluid between the inlet and the outlet of the heat sink (Fig. 8). This means that, although the fluid warms up during its path through the circuit, the system maintains a thermal flow extraction with a similar uniformity. This is a good indicator of the optimization of the design with regard to the criterion of temperature uniformity.

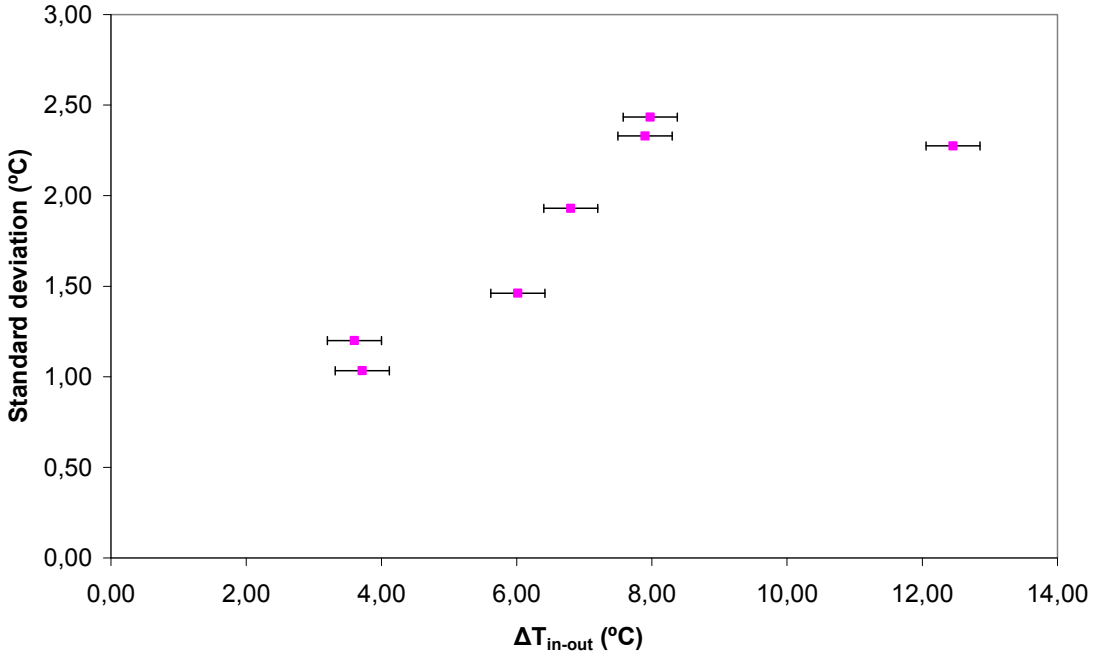

Fig. 8. Temperature uniformity at the bottom of the heat sink as a function of the difference in temperature between the points of fluid inlet and outlet. Points include uncertainty bars due to thermocouples.

4.3 Heat exchange

Calculation of the average thermal resistance coefficient R_{tm} of the system was carried out by applying the following equation:

$$R_{tm} = \frac{(T_w - T_{in})}{q''_{eff}} \qquad (10)$$

where q''_{eff} is the heat flux , T_{in} the water temperature at entry to the heat sink and T_w the average temperature of the wall on which the heat flux took place. In this study, in order to simulate the thickness of the object to be cooled, this average temperature was calculated at the first row of thermocouples ($z = z_1 = -1.6$ mm). The average thermal resistance coefficient for the four different tests conditions is presented in table 3.

Table 3
Average thermal resistance coefficient and pressure losses

	TEST 1	TEST 2	TEST 3	TEST 4	TEST 5	TEST 6	TEST 7

Q	m^3/s	2.07E-05	2.07E-05	1.32E-05	8.42E-06	1.55E-05	1.55E-05	1.60E-05
ΔP_{in-out}	Pa	702	620	318	223	435	410	470
T_W	ºC	29.9	39.5	43.1	50.5	25.9	44.1	52.2
T_{in}	ºC	12.35	12.35	12.59	12.73	12.5	12.7	29.2
q''_{eff}	W/cm^2	21.8	32	31	31	13.2	31	32
R_{tm}	$m^2.K/W$	8.1E-05	8.5E-05	9.8E-05	1.2E-05	1.0E-05	1.0E-05	7.2E-05

Fig. 9 shows the distribution of the local Nusselt number along the heat sink bottom wall. The local Nusselt number is defined as

$$Nu_x = \frac{q''\cdot d_h}{k_f \cdot (T_S - T_{in})} \tag{11}$$

where q" is the local heat flux obtained by the equation

$$q'' = -k_{Al} \cdot \frac{(T_{z_3} - T_{z_1})}{z_3 - z_1}. \tag{12}$$

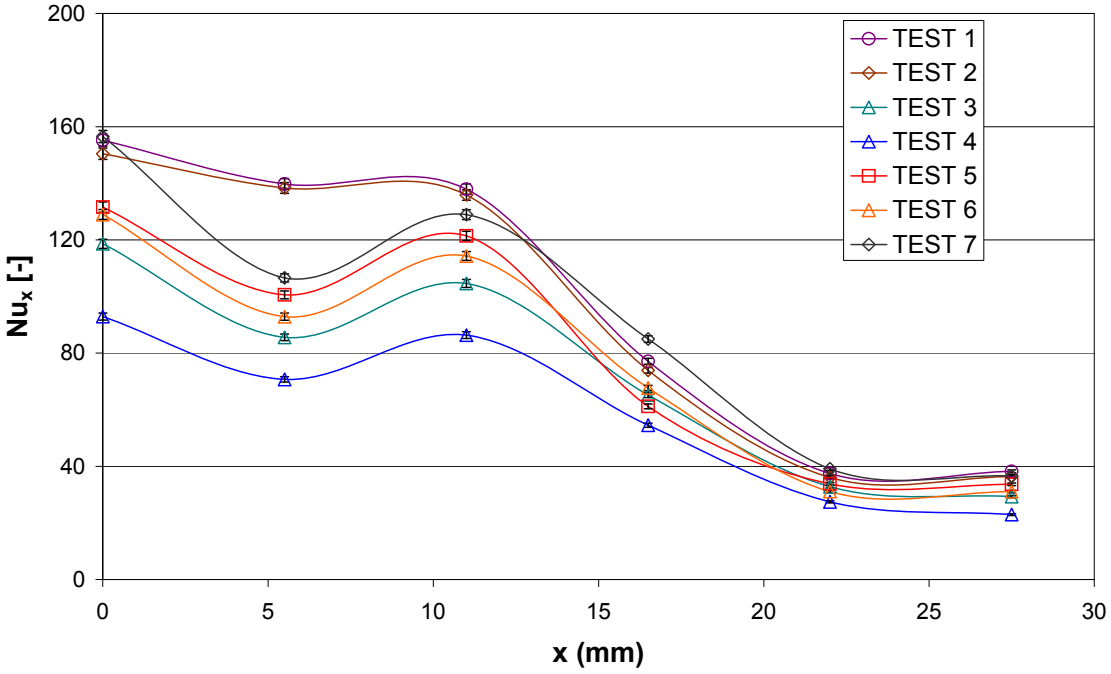

Fig. 9. Nusselt number distribution on the heat sink bottom wall. Error propagation is included in the calculation of the Nusselt number (1.36%).

The effect of jet velocity in the jet impingement influence zone is well shown with the Nusselt number distribution. Indeed, for high flow rates (test 1 and 2), the Nusselt number remains practically constant from x = 0 to 11 mm. Furthermore, it's very interesting to note that, if the local Nusselt number is multiplicated by the number of channels in each section, the results will become in a practically constant trend from x = 0 mm to x = 27,5 mm. This characteristic implies the quite uniform temperature profile at the heat sink bottom wall (Fig. 7). The local Nusselt number of the proposed hybrid jet impingement/micro-channel cooling scheme (with water as coolant fluid) is higher than the one of the hybrid micro-channel / jet impingement module calculated by Sung and Mudawar [12]. Specifically, for Re=2892, q''_{eff}=20.58 W/cm^2 with HFE-7100 as working fluid, the maximum local Nusselt number is 56.19, with higher

longitudinal (x) and transversal (y) non uniformities of the local Nusselt number distribution. In effect, the temperature uniformity of the proposed design in the y axis is assured by the proper geometry of the heat sink.

4.4 Pressure losses

Fig. 10 shows the measured pressure losses of the system for the seven tests presented. The quantitative values are lower than for micro channels devices in the same configuration. In fact, the large pressure losses of the micro-channels are due to the large contact area between the fluid and the walls of the heat sink. This implies great friction. In the proposed hybrid system, the contact area between the fluid and the walls only appears in the final part of the circuit, which implies smaller pressure losses. The increase of the pressure losses with the Reynolds number in a non-linear form was observed, according to trends derived from Moddy's diagram.

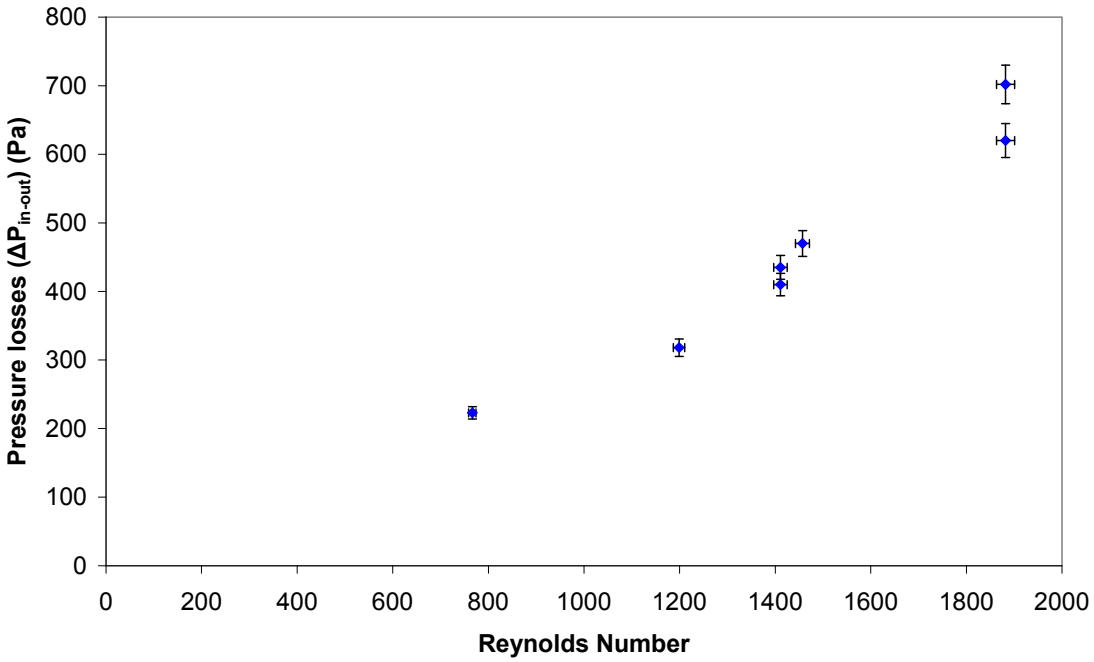

Fig. 10. Pressure losses from the cooling system. Error bars due to lack of accuracy of the pressure sensor are included.

5 Conclusion

After the analysis of the bibliography related to hybrid jet impingement / micro-channels heat sinks, a new cooling scheme has been proposed. The single-phase performance was experimentally studied in pursuit of a geometry that yields lower surface temperature and smaller temperature gradients.

The results validated the adopted solution. As well as helping to obtain high heat transfer coefficients, the combination of key parameters of each of the

thermal extraction technologies helps to improve the uniformity of temperature of the heat sink, or even to achieve specific temperature distributions adapted to the specific needs for other applications.

This study opens the way for the optimization of all the key parameters of the proposed cooling scheme (inlet velocity, channel distribution, the presence of curved surfaces under the impinging jet, channel height, etc) and towards obtaining a heat sink that provides both a very low thermal resistance and a weak temperature gradient across its base.

References

[1] S. G. Kandlikar and A. V. Bapat, "Evaluation of jet impingement, spray and microchannel chip cooling options for high heat flux removal," *Heat Transfer Engineering,* vol. 28, pp. 911-923, 2007.

[2] D. -. Lee and K. Vafai, "Comparative analysis of jet impingement and microchannel cooling for high heat flux applications," *International Journal of Heat and Mass Transfer,* vol. 42, pp. 1555-1568, 1999.

[3] K. Vafai and L. Zhu, "Analysis of two-layered micro-channel heat sink concept in electronic cooling," *International Journal of Heat and Mass Transfer,* vol. 42, pp. 2287-2297, 1999.

[4] S. H. Chong, K. T. Ooi and T. N. Wong, "Optimisation of single and double layer counter flow micro channel heat sinks," *Applied Thermal Engineering,* vol. 22, pp. 1569-1585, 2002.

[5] A. Royne and C. J. Dey, "Design of a jet impingement cooling device for densely packed PV cells under high concentration," *Solar Energy,* vol. 81, pp. 1014-1024, 2007.

[6] S. P. Jang, S. J. Kim and K. W. Paik, "Experimental investigation of thermal characteristics for a microchannel heat sink subject to an impinging jet, using a micro-thermal sensor array," *Sensors and Actuators, A: Physical,* vol. 105, pp. 211-224, 2003.

[7] D. Copeland, H. Takahira, W. Nakayama and B. Pak, "Manifold microchannel heat sinks: Theory and experiment," *American Society of Mechanical Engineers, EEP,* vol. 10-2, pp. 829-835, 1995.

[8] J. H. Ryu, D. H. Choi and S. J. Kim, "Three-dimensional numerical optimization of a manifold microchannel heat sink," *International Journal of Heat and Mass Transfer,* vol. 46, pp. 1553-1562, 2003.

[9] D. -. Lee and K. Vafai, "Comparative analysis of jet impingement and microchannel cooling for high heat flux applications," *International Journal of Heat and Mass Transfer,* vol. 42, pp. 1555-1568, 1999.

[10] S.G. Kandlikar, H.R. Upadhye, “Extending the heat flux limit with enhanced microchannels in direct single-phase cooling of computer chips”, Invited Paper presented at IEEE-Semi-Therm 21, San Jose, 15–17 March 2005.

[11] M. K. Sung and I. Mudawar, “Experimental and numerical investigation of single-phase heat transfer using a hybrid jet-impingement/micro-channel cooling scheme” *International Journal of Heat and Mass Transfer,* vol. 49, pp. 682-694, 2006.

[12] M.K. Sung, I. Mudawar, “Single-phase and two-phase cooling using hybrid micro-channel/slot-jet module” *International Journal of Heat and Mass Transfer* Volume 51, Issues 15-16, 15 July 2008, Pages 3825-3839

[13] A. J. Robinson and E. Schnitzler, "An experimental investigation of free and submerged miniature liquid jet array impingement heat transfer," *Experimental Thermal and Fluid Science,* vol. 32, pp. 1-13, 2007.